

Electric Field Control of Structure, Dimensionality, and Reactivity of Gold Nanoclusters on Metal-Supported MgO Films

Bokwon Yoon and Uzi Landman*

School of Physics, Georgia Institute of Technology, Atlanta, Georgia 30332-0430, USA

(Received 7 September 2007; published 7 February 2008)

Electric field control of the structure, dimensionality, and reactivity of gold nanoclusters (Au_{20}) deposited on MgO films of various thicknesses supported on Ag(100) are introduced and studied using first-principles electronic structure calculations. Field-controlled interfacial charging and field-induced dimensionality crossover are predicted. For a field $E_z = 1$ V/nm, an optimal planar Au_{20} island on MgO(8 layers)/Ag(100) is determined, while for $E_z = 0$, the preferred structure of the cluster is a tetrahedron. Field control of the reactivity of the adsorbed nanocluster with O_2 is discussed.

DOI: [10.1103/PhysRevLett.100.056102](https://doi.org/10.1103/PhysRevLett.100.056102)

PACS numbers: 68.47.Jn, 68.35.-p

Control of the structure and stability of nanostructures and tunability of their properties and functionalities are some of the main goals of modern research of nanoscale materials in general, and in nanocatalysis in particular [1,2]. Recently, it has been predicted theoretically [3,4], and subsequently confirmed experimentally [5], that while on the surface of bulk and thick metal-oxide films [e.g., MgO(100)] grown epitaxially on metal substrates [e.g., Mo(100) or Ag(100)], three-dimensional (3D) structures of deposited gold clusters are most stable, a dimensionality crossover occurs for thinner metal-supported oxide films (under 8 layers), with 2D planar structures gaining in stability compared to the 3D ones. The stabilization of the 2D structure (i.e., enhanced wettability of the metal-oxide thin film surface) has been found [3,4] to be caused by accumulation of electronic charge (originating from the underlying metal support) at the cluster-to-metal-oxide interface, which is enhanced by the larger interfacial contact area of the planar structure compared to the 3D one. The excess charge results in attractive interaction with its image in the underlying metal, thus binding more strongly the partially (negatively) charged adsorbed 2D metal nanostructure. Additionally, the excess charge on the gold cluster has been predicted [4] to catalyze, on sufficiently thin metal-supported MgO films, the oxidation reaction of CO to CO_2 , through activation of the adsorbed O_2 through population of the antibonding $2\pi^*$ orbital.

Here, we report on the use of external electric fields to control and manipulate the structural stability, dimensionality, and chemical reactivity of gold nanoclusters (Au_{20}) deposited on MgO films of various thicknesses, grown on an Ag(100) substrate. Employing first-principles calculations, we predict field-controlled interfacial charging and field-induced structural dimensionality crossover; e.g., for a field of 1 V/nm, we determine an optimal 2D planar configuration of an Au_{20} island adsorbed on an Ag-supported 8-layer MgO(100) film, while under field-free conditions, the preferred structure of the adsorbed Au_{20} cluster is a 3D tetrahedron. Furthermore, we illustrate

field-dependent control and tunability of the chemical reactivity of adsorbed Au nanoclusters with O_2 .

In our investigations of the electronic and geometric structures of surface-deposited nanoclusters [6], with and without an external electric field [7], we employ first-principles density-functional theory (DFT) calculations [8,9], with the use of the generalized gradient approximation (GGA) [10], ultrasoft pseudopotentials [11] (scalar relativistic ones for gold) with a plane wave basis (kinetic energy cutoff of 400 eV).

We focused here on an Au_{20} cluster which in the gas-phase has been found (through photoemission [12,13] and electron diffraction [14] measurements coupled with theoretical calculations) to exhibit an optimal tetrahedral structure, $\text{Au}_{20}(T)$, with a sizeable energetic advantage $\delta E_{\text{gas}}(T, P) = E[\text{Au}_{20}(P)] - E[\text{Au}_{20}(T)] = 1.95$ eV over the corresponding planar isomer, $\text{Au}_{20}(P)$. The 3D tetrahedral structure maintains its excess stability over the 2D one when adsorbed on a bulk MgO(100) surface. On the other hand, as noted above, for sufficiently thin films (under 8 layers) of MgO(100) epitaxially supported on metals [Mo(100) or Ag(100)], a planar structure of Au_{20} shows excess stability [3–5].

To quantify the thickness-dependent stabilization effect, we define the cluster binding energy (BE) to the surface as $(\text{BE})_n[\text{Au}_{20}(T/P)] = E_{\text{gas}}[\text{Au}_{20}(T/P)] + E[(\text{MgO})_n/\text{Ag}] - E[\text{Au}_{20}(T/P)/(\text{MgO})_n/\text{Ag}]$, where $E[\dots]$ denotes the total energy (<0) of the relaxed system, (T/P) denote tetrahedral or planar structure of the adsorbed Au_{20} cluster, and n is the number of layers of the metal-supported MgO film. All the results were obtained following unconstrained structural optimization. We also define the charge difference, ΔQ_n [$\text{Au}_{20}(T/P)$], between the total electronic charge of the combined system $\text{Au}_{20}(T/P)/(\text{MgO})_n/\text{Ag}(100)$, optimized with (or without) an external electric field, and the isolated cluster and surface support kept in the geometry as in the combined system. Figures 1(a) and 1(b) reveal notable dependencies of $(\text{BE})_n$ and ΔQ_n on the MgO film thicknesses for the

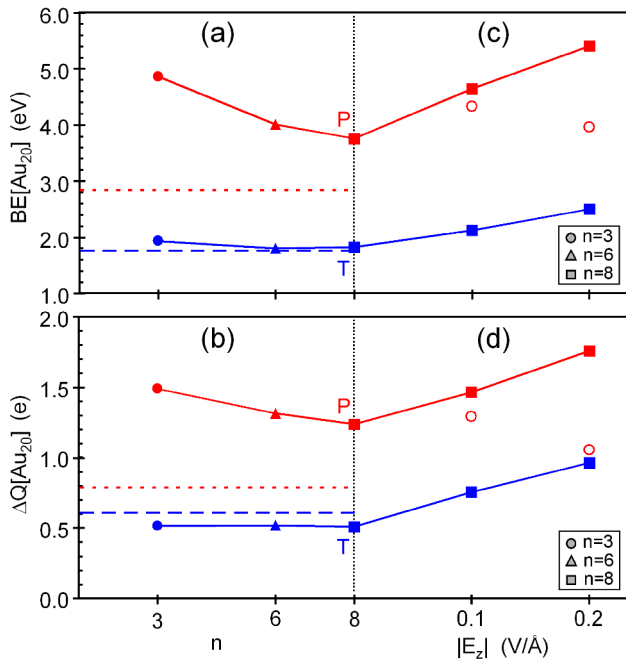


FIG. 1 (color online). Binding energies and excess electronic charges for adsorbed Au₂₀ clusters; in (a)–(d) upper curves and lower curves correspond, respectively, to planar, Au₂₀(P), and 3D, Au₂₀(T), clusters. In (a) and (b), (BE)[Au₂₀] and ΔQ[Au₂₀] are shown versus the number of MgO layers, n , supported on Ag(100) under field-free conditions, and in (c) and (d), they are shown, for clusters adsorbed on an Ag-supported 8-layer MgO films, as a function of the external electric field strength. Dotted and dashed lines denote (BE)[Au₂₀] and ΔQ[Au₂₀] for the planar and tetrahedral clusters, respectively, adsorbed on the surface of bulk MgO films (without metal support). Values for Au₂₀(P)/MgO(3L)/Ag(100), displayed in (c) and (d) by empty (red) circles, are for the reversed field polarity, i.e., $E_z = -0.1$ V/Å and -0.2 V/Å, showing reduced BE and ΔQ; compare to the $E_z = 0$ results shown in (a) and (b).

adsorbed planar (2D) structures [see upper curves in (a)–(d)]. In contrast, the results for the 3D structures show relative insensitivity to n [see lower curves in (a)–(d)].

We also define the binding energy difference for the two structures of the adsorbed clusters $\delta(\text{BE})_n[\text{Au}_{20}(T, P)] = (\text{BE})_n[\text{Au}_{20}(P)] - (\text{BE})_n[\text{Au}_{20}(T)]$, and the binding energy difference normalized to the energy difference between the gas-phase T and P structures, i.e., $\Delta E_n[\text{Au}_{20}(T, P)] = \delta(\text{BE})_n[\text{Au}_{20}(T, P)] - \delta E_{\text{gas}}[\text{Au}_{20}(T, P)]$; note that for $\Delta E_n[\text{Au}_{20}(T, P)] < 0$, the adsorbed 3D structure (T) is energetically favored, while the planar 2D structure (P) is preferred for positive values of ΔE_n . In Fig. 2(a), we display calculated values of $\Delta E_n[\text{Au}_{20}(T, P)]$, showing dominance of the 2D adsorbed structure for $n = 3$ and 6, with the 3D tetrahedral structure emerging as the favored one for supported MgO films with $n \geq 8$ layers, $\Delta E_8[\text{Au}_{20}(T, P)] = -0.02$ eV. As aforementioned, the 3D tetrahedral structure is favored for all thicknesses of

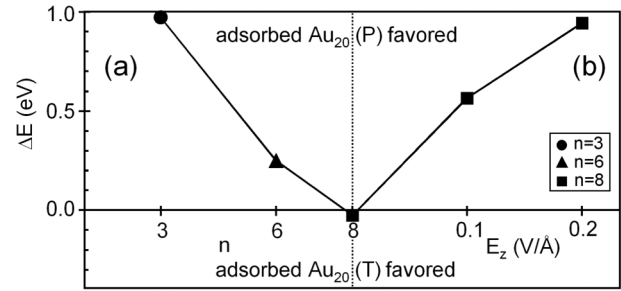


FIG. 2. Binding energy differences normalized to the energy difference between the tetrahedral and planar structures in the gas phase (see text). (a) ΔE plotted vs n , the number of MgO(100) layers supported on Ag(100), with $E_z = 0$. (b) ΔE vs E_z calculated for Au₂₀ adsorbed on MgO(8L)/Ag(100). Lines connect the calculated values to show the trend.

free standing MgO(100) films, with $\Delta E[\text{Au}_{20}(T, P)] = -0.87$ eV calculated for a 6-layer film.

Application of an electric field cancels the thickness-dependent dimensionality crossover found above for the field-free case. Indeed, the dominance of the planar adsorbed structure, Au₂₀(P), is restored under the influence of a field applied to the 8-layer MgO film [see Fig. 2(b)]. The field-induced increased wetting propensity [Figs. 1(c) and

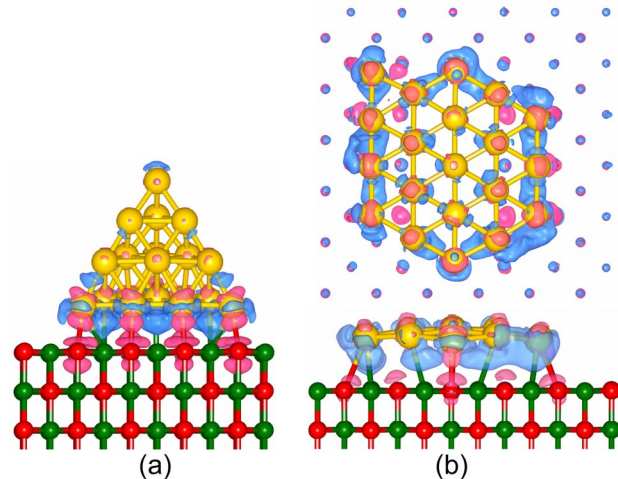


FIG. 3 (color online). Isosurfaces of electronic charge differences shown as shaded regions localized mainly at the cluster/surface interface [see (a) and bottom figure in (b)], calculated for the system Au₂₀(T/P)/MgO(8L)/Ag(100) and optimized with an external electric field of 0.1 V/Å (on line the excess charge is in blue and the charge depletion is pink). The isosurfaces are superimposed on the atomic structure; oxygen and Mg atoms of the surface are depicted as darker spheres (online red and green, respectively), and the gold atoms of the adsorbed cluster are depicted as gray shaded spheres (online yellow). (a) a 3D tetrahedral adsorbed cluster isomer, and (b) the energetically favored planar adsorbed cluster, with a top view given above (the surface atoms are not displayed), illustrating preferable charging at the island periphery, and a side view shown at the bottom.

2(b)] is accompanied by enhanced interfacial charge accumulation as shown in Fig. 1(d). The spatial distribution of the accumulated charge is visualized in Fig. 3.

Interestingly, our calculations predict the ability to manipulate the wettability of the substrate also via reversal of the applied field direction (polarity). This effect is illustrated for $\text{Au}_{20}(P)/\text{MgO}(3\text{L})/\text{Ag}(100)$ through calculations with $E_z = -0.1$ and -0.2 V/\AA [see open circles in Figs. 1(c) and 1(d)], where 3L denotes three layer. We find for the two fields, respectively, binding energies (and charge excess) of 4.33 eV ($1.29e$) and 3.96 eV ($1.06e$), which are both smaller than the ones calculated in the absence of the electric field, i.e., $(\text{BE})_3[\text{Au}_{20}(P)] = 4.86 \text{ eV}$ and $\Delta Q_3[\text{Au}_{20}(P)] = 1.49e$.

The ability to control and tune the chemical activity of nanocatalysts through the use of applied electric fields is particularly interesting. To this aim, we have compared certain characteristics of adsorbed molecular oxygen on surface-supported Au_{20} clusters, under field-free conditions and in the presence of applied fields. For reference, we note first that for a thin (three-layer) MgO film supported on Ag(100), the Au_{20} cluster, which takes a favorable planar geometry, adsorbs O_2 at the cluster periphery with a binding energy of 0.8 eV, with the adsorbed molecule in an activated peroxy state, having spin $S = 0$ and an internuclear distance $d_{\text{OO}} = 1.45 \text{ \AA}$, compared to 1.26 \AA in the paramagnetic gas-phase oxygen molecule; binding of the molecule to the energetically less favorable (by close to 1 eV) 3D tetrahedral gold cluster occurs also at the interface of the cluster with the MgO surface, with an adsorption energy of 0.24 eV and an activation of the molecule to a peroxy state with $d_{\text{OO}} = 1.43 \text{ \AA}$.

As noted above, on a thicker metal-supported 8-layer thick MgO film, the 3D cluster is (slightly) energetically favored, and it is found to adsorb molecular oxygen relatively weakly (a binding energy of 0.19 eV at the top apex of the tetrahedron) with the molecule maintaining a non-activated ($d_{\text{OO}} = 1.275 \text{ \AA}$) $S = 1$ state; the adsorption energy to the corresponding planar gold cluster is higher (0.85 eV), and the molecule is activated ($d_{\text{OO}} = 1.43 \text{ \AA}$ and $S = 0$). Interestingly, under the effect of an electric field of 0.2 V/\AA , the binding of the O_2 molecule to the 3D adsorbed cluster increases to 0.37 eV with the molecule bound to the cluster (at the cluster interface with the MgO surface) in an intermediate superoxy or peroxy state ($S = 0$ and $d_{\text{OO}} = 1.41 \text{ \AA}$). Under the same conditions, binding to the (now) favored 2D cluster increases to 0.98 eV, with the molecule in a highly activated peroxy state ($S = 0$ and $d_{\text{OO}} = 1.44 \text{ \AA}$).

The field-induced modifications of the electronic structure, atomic arrangements, and dimensionality of surface-supported metal nanoclusters, introduced and illustrated here, suggest new research avenues on nanostructures and nanocatalysis. Implementation of external field control and tunable manipulations of the physical and chemical

properties of nanostructures remain an outstanding experimental challenge.

Research supported by the US AFOSR and the US DOE. Computations performed at the Georgia Tech Center for Computational Materials Science and the National Energy Research Computational Center (NERSC) at the Lawrence Berkeley Laboratory, Berkeley, CA.

*Corresponding Author: uzi.landman@physics.gatech.edu

- [1] U. Heiz and U. Landman, *Nanocatalysis* (Springer, New York, 2006).
- [2] U. Landman, B. Yoon, C. Zhang, U. Heiz, and M. Arenz, *Top. Catal.* **44**, 145 (2007).
- [3] D. Ricci, A. Bongiorno, G. Paccioni, and U. Landman, *Phys. Rev. Lett.* **97**, 036106 (2006).
- [4] C. Zhang, B. Yoon, and U. Landman, *J. Am. Chem. Soc.* **129**, 2228 (2007).
- [5] M. Sterrer, T. Risse, M. Heyde, H.-P. Rust, and H.-J. Freund, *Phys. Rev. Lett.* **98**, 206103 (2007).
- [6] MgO films were modeled by placing n MgO layers ($n = 3, 6,$ and 8) on top of 4 layers of an Ag(100) surface with a lattice constant of 2.94 \AA (about 2% smaller than the calculated bulk MgO lattice constant). The two bottom Ag layers were held fixed, while the rest of the system was structurally optimized using a conjugated gradient relaxation method. When investigating adsorption on an unsupported MgO surface, 6 layers of MgO (100) with bulk interlayer spacing were used, and the bottom layer was held fixed during structural optimizations. For an adsorbed tetrahedral gold cluster $[\text{Au}_{20}(T)]$, having an interfacial facet of 10 gold atoms, a 5×5 MgO(100) cell (with 25 Mg and 25 O atoms per layer) was used, while for an adsorbed planar Au cluster $[\text{Au}_{20}(P)]$, we used 6×6 MgO (100) layers (36 Mg and 36 O atoms in each layer). The number of atoms (per layer) in the silver substrate underlying the MgO film was 25 for the case of an adsorbed tetrahedral gold cluster, and 36 for the case of a planar one. A 20 \AA thick vacuum region was used to separate the periodically replicated slabs (with a thicker region used when applying an external field). The large size of the computational supercell used by us [up to 6×6 larger than the planar unit cell of the MgO(100) and Ag(100) substrate, i.e., equivalent to a 6×6 k -point sampling when a single planar unit cell is used for the substrate] justifies the $k = 0$ (Γ -point sampling) calculations that we employed here. Comparisons between the $k = 0$ calculations and test computations that included explicit k -point sampling ($2 \times 2 \times 1$ and $4 \times 4 \times 1$, i.e., increasing the effective number of k points up to $24 \times 24 \times 1$) provided clear evidence that the $k = 0$ results are indeed well converged, with differences in total energies well below 1%, and differences (in comparison with the $k = 0$ results) of at most 1% between the binding energies. We conclude that added k -point sampling has no discernible effect on the results of our computations.
- [7] A homogeneous external electric field, E_z was applied using the method of K. Kunc and R. Resta, *Phys. Rev. Lett.* **51**, 686 (1983). A field, E_z^* of the opposite sign was

applied in the vacuum region of the supercell, that is, $E_z^* = -[(Z_{\max} - L)/L]E_z$ where Z_{\max} is the length of the supercell and L is the length of the region where the reversed field is applied. Sufficiently large L was used to prevent electronic charge localization in the vacuum region. Faster convergence was achieved with a sinusoidal smoothing function applied in a 2 Å wide zone connecting the two field regions.

- [8] G. Kresse and J. Hafner, Phys. Rev. B **47**, 558 (1993).
- [9] G. Kresse and J. Furthmuller, Phys. Rev. B **54**, 11169 (1996).
- [10] J.P. Perdew, J.A. Chevary, S.H. Vosko, K.A. Jackson, M.R. Pederson, D.J. Singh, and C. Fiolhais, Phys. Rev. B **46**, 6671 (1992).
- [11] D. Vanderbilt, Phys. Rev. B **41**, 7892 (1990).
- [12] J. Li, X. Li, H.-J. Zhai, and L.-S. Wang, Science **299**, 864 (2003).
- [13] B. Yoon, P. Koskinen, B. Huber, O. Kostko, B. Issendorff, H. Häkkinen, M. Moseler, and U. Landman, Chem. Phys. Chem. **8**, 157 (2007).
- [14] X. Xing, B. Yoon, B. U. Landman, and J.H. Parks, Phys. Rev. B **74**, 165423 (2006).